LIBRARY
Michigan State
University

This is to certify that the
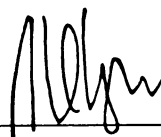
thesis entitled

**TAILORING MATERIALS WITH PRESCRIBED CONSTITUTIVE
PARAMETERS USING POLYGONAL CELLS**

presented by

Weian Ou

has been accepted towards fulfillment
of the requirements for

_____MS_____degree in Mechanical Engineering

_____
Major professor

Date **11 DEC, 2001**

O-7639   *MSU is an Affirmative Action/Equal Opportunity Institution*

PLACE IN RETURN BOX to remove this checkout from your record.
TO AVOID FINES return on or before date due.
MAY BE RECALLED with earlier due date if requested.

DATE DUE	DATE DUE	DATE DUE

TAILORING MATERIALS WITH PRESCRIBED CONSTITUTIVE PARAMETERS USING POLYGONAL CELLS

By

Weian Ou

A THESIS

Submitted to
Michigan State University
in partial fulfillment of the requirements
for the degree of

MASTER OF SCIENCE

Department of Mechanical Engineering

2001

ABSTRACT

TAILORING MATERIALS WITH PRESCRIBED CONSTITUTIVE PARAMETERS USING POLYGONAL CELLS

By

Weian Ou

The topic of this thesis is to use the topology optimization method to solve an inverse homogenization problem in which the micro-geometry of a composite (characterized by a polygonal cell) made of two constituents is designed to match a set of prescribed elastic properties. In this thesis, we also investigate whether using polygonal cells in the homogenization procedure can result in materials that reach extremal properties.

The effect of different starting points is investigated. The results show that different starting points will lead to different answers with the same target tensor, which points at the non-unique of the solution. The question whether different shape parallelograms can lead to different answers matching the same target tensor is examined. The results show that one can achieve different microstructure that match the desired target tensor by changing the geometry of the base cell. We study the effect of changing of the amount of available material. The results show clearly that different volumes of strong material can generate different answers that match the same elastic tensor. The results obtained are close to the lower right corner of the Hashin-Shtrikman bounds.

ACKNOWLEDGMENT

I would like to thank my advisor Prof. Alejandro Diaz for guidance, along with my committee, Profs. Andre Benard, and Farhang Pourboghrat. Sudarsanam Chellappa provided me with the assistance in testing the program. I also would like to thank Nader Abedrabbo for his help on my programming work in Matlab.

TABLE OF CONTENTS

LIST OF FIGURES

Chapter 1

INTRODUCTION

Composite materials are becoming increasingly important in industry. The weight and strength ratio of these materials makes them suitable for a large variety of applications. The application of the composite material determines what kind of property it should have. The purpose of this thesis is to use the topology optimization method to solve an inverse homogenization problem in which the micro-geometry of a composite made of two constituents is designed to match a set of prescribed elastic properties. In this thesis, we also investigate whether using polygonal cells in the homogenization procedure can result in materials that reach extremal properties.

1.1 Inverse Homogenization

The goal of an inverse homogenization problem is to find a (periodic) microstructure in which the infinitly small-scale mixture of two constituents forms a composite material whose effective elastic tensor matches some arbitrarily prescribed values. The inverse homogenization problem here deals with linear elastic materials and small deformation kinematics in both macroscopic and the microscopic scales. It can be shown that after using the homogenization procedure, the constitutive parameters can be expressed as explicit functions of a finite number of parameters. The inverse homogenization problem can thus be formed as an optimization problem to possibly minimize the deviation from

the target tensor with a prescribed amount of material. We can then use the topology optimization method to solve it.

Sigmund (1994) solved the inverse homogenization by using square or rectangular base cells only. Although this is not a fundamental constraint, this restriction can be released by using polygonal cells without significant additional numerical complexity. It will increase the design space remarkably by using polygonal cells to solve the inverse homogenization problem. In Sigmund (1999), the inverse homogenization problem is solved to find a new class of extremal composites. Also in this work only the square cells are used and the bound of lower shear modulus is reached. The idea of using the polygonal cell is inspired by Benard and Diaz (2001). In that paper, features related to the discretization of problems characterized by simple periodic tiling using cells of various shapes are discussed. The paper shows that various cell geometries capable of tiling the plane can be replaced by an equivalent problem where the plane is tiled by polygonal base cells. The base cell will be discretized with finite elements. The result of the inverse homogenization will be presented as an optimized geometric distribution of the two constituents in the base cell.

1.2 Topology Optimization

Topology optimization of plane structures involves the determination of features such as the number and location of holes and the connectivity of the domain. In the inverse homogenization problem, the goal is to allocate the prescribed volume fraction in the

2

design domain to make its elastic tensor meet the arbitrarily prescribed elastic tensor, or target tensor.

Composites can be designed to have many physical properties, such as Young's modulus, Poison's ratio, shear modulus, bulk modulus, conductivity, etc. Composite materials with extreme properties (e.g., the "stiffest" composite) are very important in material science and structural optimization. They can be used to establish bounds for structural performance and are widely used in the field of topology optimization. Bendsoe, Guedes, Haber, Pedersen, and Taylor (1994) answered in analytical form the question "what is the optimal configuration of material throughout a structure that is consistent with the objective for globally optimal design". In that paper, they show that the measure of compliance predicted in their formulation bounds from below the compliance of similar structure, which presented in the paper, relative to all possible material configurations. Bendose, and Kikuchi (1988) use composite mixtures to produce a methodology for optimal shape design that avoids drawbacks that affect "traditional" shape optimizations. One such drawback is that the optimal shape design of structural elements based on boundary variations results in final designs that are topologically equivalent to the initial choice of design. Thus, the region of the design space explored by such method is limited. Another drawback is that general stable computational schemes for standard shape optimization often require some kind of remeshing of the finite element approximation of the analysis problem.

1.3 Extreme Properties

The elastic tensor of an <u>isotropic</u> material, which is composed by mixing two isotropic

constituents can be described by its effective bulk modulus k^* and its shear modulus μ^*.

Considering two isotropic constituents with bulk and shear moduli denoted by k^1, k^2,

μ^1 and μ^2, respectively, if the constituent with larger bulk modulus also has the larger

shear modulus ($\left(k^2 - k^1\right)\left(\mu^2 - \mu^1\right) \geq 0$), the two constituents are called "well-ordered".

Otherwise they are called non-well-ordered ($\left(k^2 - k^1\right)\left(\mu^2 - \mu^1\right) < 0$). There exist bounds

of the effective bulk modulus and effective shear modulus that this kind of composite

material can reach. The first bound was given by Hill(1952). Later, these bounds were

improved by Hashin and Shtrikman (1963) for three-dimensional composites and well-

ordered constituents. Hashin and Shtrikman (1963) applied variation principles, involving

the elastic polarization tensor, to derive the upper and lower bounds for the effective

elastic moduli of the materials described as mechanical mixtures of a number of different

isotropic and homogeneous elastic phases.

The bounds for the non-well-ordered case were then improved by Walpole (1966).

Walpole presented general bounds for both well-ordered and non-well-ordered cases, as

Hashin and Shtrikman (1963) only considered the well-order case. Subsequently, Milton

and Phan-Thien (1982) and Berryman and Milton (1988) set up new bounds on the

effective moduli of a two-constituent-composite material. Milton and Phan-Thien (1982)

showed in detail how Hashin and Shtrikman's (1963) bounds can be extended and how

Walpole's (1966) bounds can be improved using two inequalities on the two geometrical

parameters that appear in the third-order bounds on the effective shear modulus. In

Berryman and Milton (1988), examples of bounds on one effective material property

from measurements of another are derived. These examples are somewhat more

restrictive than the Hashin-Shtrikman bounds. Cherkaev and Gibiansky (1993) improved

these bounds by the translation method. The set of the bulk modulus and the shear

modulus pairs turns out to be bounded in the plane of the values of these moduli by

straight lines and also by two fractional linear curves. Sketches of the Hashin-Shtrikman

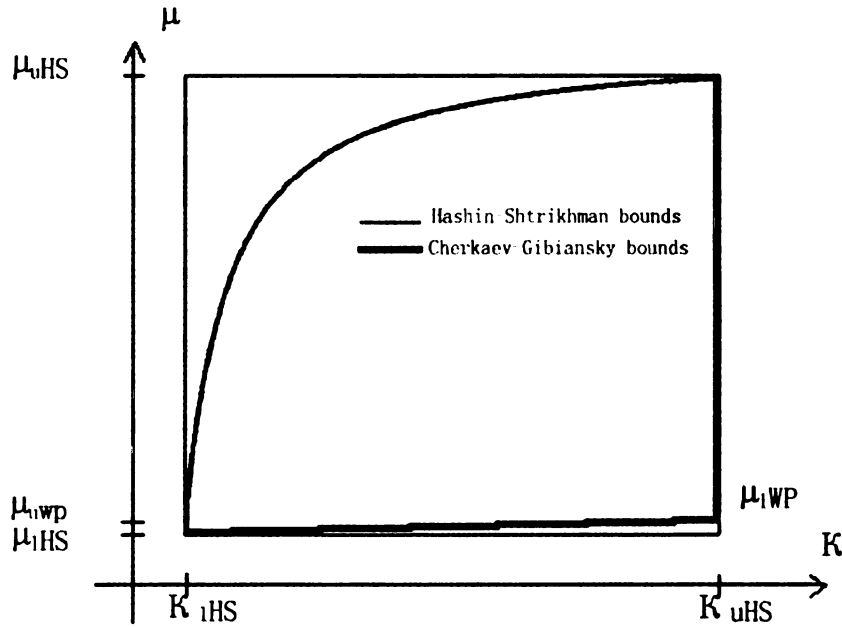and Cherkaev-Gibiansky bounds for well-ordered case are shown in Figure 1.1.

Figure 1.1. Plot of the theoretical bounds on effective bulk modulus and shear modulus for isotropic two-phase linear elastic well-ordered materials (Sigmund (1999)).

If there exist composites that attain the bounds, the effective properties of such composites are said to be optimal. An interesting question is whether one can identify the micro-geometry of composite materials that can attain the bounds. The first microstructure attaining the maximum bulk modulus bound was the spheres model composite presented by Hashin (1962). Francfort and Murat (1986) focused their attention on the mixture of two isotropic materials in prescribed volume fractions and strived to characterize all possible macroscopically isotropic composites. They produced a multi-layered composite with a finite number of element of layering directions. The results they gave proved that Hashin-Shtrikam bounds on the bulk and shear moduli can be achieved and suggested that the bounds can even be simultaneously achieved by multiple layering. Two-dimensional square symmetric rank-2 laminations attain the upper and lower bounds of the bulk modulus. Isotropic rank-3 laminations can attain the maximum bulk and shear modulus simultaneously (upper right corner of the Figure 1.1) and attain the lower-left corner of Figure1.1 by inversing the two constituents. Lutie and Cherkaev (1984) developed a method for the calculation of the extreme conductivity. The method is based on the principle of the consecutive assembling of binary mixtures through the addition of infinitely small amounts of one of the initial compounds to the already-assembled isotropic composite. The process is assumed to produce an optimal isotropic binary mixture at each step, which is performed by the Hashin-Shtrikman procedure. They suggested that the same method can be used in the optimal design of elastic constructions. In other words, there exist finite rank laminates that can attain the bulk-shear muduli bounds. Milton (1992) produced examples of composites that can be rigorously proved to have low-bulk and high-shear moduli. He found a family of two-

6

dimensional, two-phase, composite materials with hexagonal symmetry with Poison's ratios close to −1. He also showed that elastically isotropic two-dimensional composites with Poisson's ratio approaching −1 can be generated simply by layering the component materials together in different directions on widely separated length scales. In Milton and Cherkaev (1995), for a two-phase composite comprised of a sufficiently compliant, isotropic phase and a sufficiently rigid, isotropic phase, the effective elasticity tensor can realize any given definite tensor satisfying the usual symmetries of elastic tensors. This means that the optimal bulk and shear moduli bounds can be attained by this kind of composite material.

Composite with extremal properties such as rank-2 laminations are multi-scale mixtures. Instead of using the multi-length scale microstructures, Grabovsky and Kohn (1995) used the "Vigdergauz microstructure" to obtain the two-dimensional square symmetric composites with optimal shape of single inclusions. The composite is spatially periodic, consisting of properly shaped elastic inclusions embedded in an elastic matrix. Vigdergauz (1999) provided an alternative discussion of "Vigdergauz microstructure" and its properties. He also presented an analysis of various limits of the inclusion and extended the results of Grabovsky and Kohn to isotropic material. Sigmund (1993, 1994) used a numerical topology optimization approach to solve the material designing problem with extremal elastic properties. In his paper, examples of two-dimensional, two-phase microstructures with extemal bulk modulus are obtained by the inverse homogenization procedure. Ole Sigmund, (1999) tried to produce the isotropic material microstructure with maximum bulk modulus and minimum shear modulus. The results get very close to

the lower bound but have not attained it. In this thesis we will try to find out whether a two-dimensional microstructure with a periodicity characterized by arbitrary polygonal cells can attain the lower shear bound.

1.4 Periodic homogenization

In the 1970's, much research focused on defining the equivalent mechanical properties of composite materials and on determining their dependence on the difference components. Some of the methods used in that research were based on engineering. They often show a good agreement with each other's experimental data or with empirical methods. In Hashin's (1970) paper, a survey in this approach is provided. At the same time, the counterpart of such engineering methods in mathematics appears under the name of homogenization theory. This theory has been the object of large amounts of research in the area of applied mathematics. A few examples are Lions (1981) and Oleinik (1984). A homogenization method as proposed by Guedes et al.(1990) can be used to calculate the effective constitutive parameters of complex materials.

In homogenization theory, the composite material is assumed to be locally formed by the spatial repetition of microstructures infinitely small, when compared with the overall 'macroscopic' dimensions of the structure of interest. The microstructure is called 'microscopic' cells, or base cells. In other words, it is assumed that the material properties are periodic functions of the microscopic variable, where the period is infinitely small compared with the macroscopic variable. The assumption enables the

computation of equivalent material properties by computation of the material property of the base cell.

The homogenization procedure has been discussed several times in literature. One way to solve the homogenization problem is analytical calculation. For example, Aboudi and Jacob (1991) present the way to provide the overall behavior of composite materials by the micro-mechanical analysis from the known properties of the individual constituents (e.g. fibers and matrix).When more complicated microstructure need to be considered, analytical homogenization becomes too complex to be calculated. In this condition, numerical method based on the finite-element must be used. Guedes and Kikuchi (1990) presented an effective numerical homogenization procedure with adaptive finite elements methods. In this thesis, a modified version of this algorithm associated with element mutual energy will be used.

This thesis is divided into 6 chapters. Chapter 2 will describe the homogenization method. Chapter 3 will discuss relevant features and concepts related to tiling two-dimensional domains using different polygonal base tiles. Chapter 4 will describe the inverse homogenization method. Chapter 5 will present examples of inverse homogenization problem solved and discuss whether it is possible to attain the lower shear modulus bound. Chapter 6 will present conclusions and summarize the work that has been done.

Chapter 2

HOMOGENIZATION

In this chapter, basic concepts in homogenization theory relevant in this work will be briefly reviewed. Consider a composite material formed by the spatial repetition of a base cell made of two constituents, as shown in Figure 2.1. The figure presents a two-dimensional case. We assume that the mixture is represented by a base cell that is very
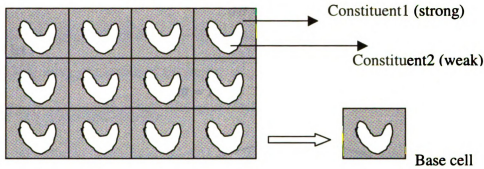

Figure 2.1. Composite structure

small (of order ε) compared with the dimensions of the body. As a result of the rapid variation of material properties, when the body is subject to some load, the resulting deformation and stresses vary rapidly from point to point. These quantities have two explicit spatial dependences: on the macroscopic scale variable x and on the small scale $y = x / \varepsilon$. Because of the periodic nature of the microstructure, the dependence of these functions on the microscopic variable $y = x / \varepsilon$ is also periodic. However, discretization of the finite scale would be impossible, e.g. using finite element methods. It is therefore necessary to develop a method that averages the microscopic structure whenever the

mechanical behavior of the macroscopic body is in question. The homogenization method is such a method.

Let Ω be an open subset of $\mathbf{R}^2$ with a smooth convex boundary Γ. Let Y be an open rectangle in $\mathbf{R}^2$ (Figure 2.2), defined as

$$Y =]0, y_1^0[\times]0, y_2^0[\tag{2.01}$$

Later in this thesis this will be generalized so that Y can be any polygonal shape that tiles the plane. Let ϑ be an open sub set of Y with boundary

$$\partial \vartheta = S \tag{2.02}$$

and let

$$\varpi = Y \setminus \overline{\vartheta} \tag{2.03}$$

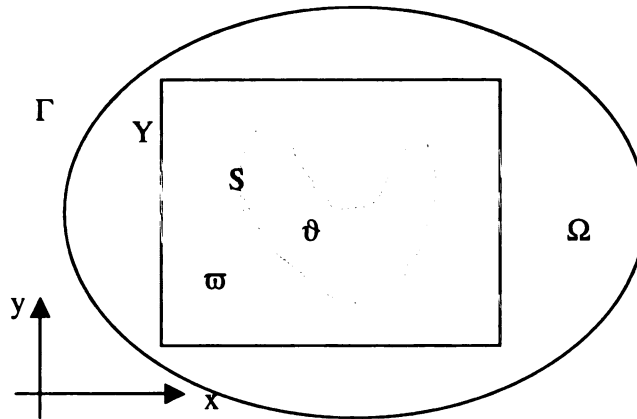
Figure 2.2. Model of the base cell

In our problem ϖ is the area occupied by the strong material. The closure of ϑ, denoted by $\overline{\vartheta}$, is the area occupied by weak material, and Y represents the base cell of the

composite microstructure. The material properties vary inside Y and are defined using the following indicator function.

$$\Theta(y) = \begin{cases} 1 & \text{if} \quad y \in \varpi, \\ 0 & \text{if} \quad y \notin \varpi, \end{cases} \tag{2.04}$$

We can then define

$$\Omega^\varepsilon = \left\{ x \in \Omega \mid \Theta(x/\varepsilon) = 1 \right\} \tag{2.05}$$

as the subset of the domain Ω occupied by the strong material and

$$S^\varepsilon = \bigcup_{\alpha=1}^{Number \ of \ cells} S_\alpha \tag{2.06}$$

as the "boundaries" between strong and weak materials.

The following assumptions are made:

1. Ω^ε is a connected domain.

2. In all cells the weak material part ϑ has sufficient smooth boundary S.

3. None of the boundary S intersects with the boundary Γ of Ω.

Let

$$V^\varepsilon = \left\{ v \in (H^1(\Omega^\varepsilon))^2 \mid v \mid_{\Gamma_d} = 0 \right\} \tag{2.07}$$

where $v \mid_{\Gamma_d}$ is the value of v on the boundary Γ_d. The problem of the deformation of a structure body Ω^ε subjected to body force f and tractions t on the boundary Γ_t with the tractions p inside the boundary S^ε, and prescribed displacement on Γ_d, can be stated as

Find $u^\varepsilon \in V^\varepsilon$, *such that*

$$\int_{\Omega^\varepsilon} E_{ijkl}^\varepsilon \frac{\partial u_k^\varepsilon}{\partial x_l} \frac{\partial v_i}{\partial x_j} d\Omega = \int_{\Omega^\varepsilon} f_i^\varepsilon v_i d\Omega + \int_{\Gamma_t} t_i v_i d\Gamma + \int_{S^\varepsilon} p_i^\varepsilon v_i ds \quad \forall v \in V^\varepsilon \tag{2.08}$$

Here strain-stress relation is

$$\left\{ \sigma^\varepsilon \right\} = \left[E^\varepsilon \right] \left\{ \epsilon^\varepsilon \right\} \tag{2.09}$$

where the elastic tensor matrix is given in the standard engineering form, i.e., E^ε is

written as

$$[E] = \begin{bmatrix} E_{1111} & E_{1122} & E_{1112} \\ E_{1122} & E_{2222} & E_{2212} \\ E_{1112} & E_{2212} & E_{1212} \end{bmatrix} \tag{2.10}$$

The conditions for existence of a unique solution u^ε to problem (2.08) is given in Necas

and Hlavacek (1981), and require that the functions f, t, and p be sufficiently smooth,

and that the boundaries Γ_d, Γ_t, and S^ε be regular.

The solution u^ε should depend on both x and y, i.e.,

$$u^\varepsilon = u(x, y), \quad y = x/\varepsilon \tag{2.11}$$

In the neighborhood of a fixed macroscopic point x it is assumed that there is a very large

number of micro-scale cells, which are obtained as copies of a base cell. Dependence on

y can be considered periodic or Y-periodic, at a fixed point x in the microscopic level.

Furthermore, it is assumed that the form of the base cell varies in a smooth way as the

macroscopic variable x changes. This means that at different points x the composite

structure may vary, but a periodic pattern can always be found in a microscopic

neighborhood of point x.

13

Since the solution u^{ε} depends on both macroscopic and microscopic variables, it is reasonable to assume that u^{ε} can be expressed as an asymptotic expansion with respect to the parameter ε (the "scale", or the ratio of microscopic/macroscopic dimensions), i.e.,

$$u^{\varepsilon} = u^0(x, y) + \varepsilon u^1(x, y) + \varepsilon^2 u^2(x, y) + ..., \qquad y = x/\varepsilon \qquad (2.12)$$

where

$$u^j(x, y) \text{ is defined on } (x, y) \in \Omega \times \varpi \qquad (2.13)$$

$$u^j(x, y) \text{ is Y-periodic}$$

In order to find the homogenized elastic constants such that the macroscopic equilibrium can be described by the same equation as (2.08), let $\chi_p^{(kl)} \in V$ be the solution of

$$\int_Y E_{ijpq} \frac{\partial \chi_p^{kl}}{\partial y_q} \frac{\partial v_i}{\partial y_j} dY = \int_Y E_{ijkl} \frac{\partial v_i}{\partial y_j} dY \qquad \forall v \in V \qquad (2.14)$$

$$V = \left\{ v \in (H^1(\Omega))^2 : v \quad is \quad Y - periodic \right\}$$

and let $\psi_k \in V$ be the solution of

$$\int_Y E_{ijkl} \frac{\partial \psi_k}{\partial y_l} \frac{\partial v_i}{\partial y_j} dY = \int_S p_i v_i(y) dY \qquad \forall v \in V \qquad (2.15)$$

If only the first order terms of the u^{ε} asymptotic expansion are considered, it can be shown (Sigmund 1994) that the global elastic constants of the material are given by

$$E_{ijkl}^H = \frac{1}{Y} \int_Y \left[E_{ijkl} - E_{ijpq} \frac{\partial \chi_p^{kl}}{\partial y_q} \right] dY \qquad (2.16)$$

14

This equation represents the macroscopic equilibrium, while E_{ijkl}^H represents the

homogenized elastic constants, i.e.,

$$\int_\Omega E_{ijkl}^H \frac{\partial u_k^0}{\partial x_l} \frac{\partial v_i}{\partial x_j} d\Omega =$$

$$\int_\Omega (\frac{1}{|Y|} \int_Y f_i dY) v_i d\Omega + \int_{\Gamma_t} t_i v_i d\Gamma + \int_\Omega (\frac{1}{|Y|} \int_Y E_{ijkl} \frac{\partial \psi_k}{\partial y_l} dY) \frac{\partial v_i}{\partial x_j} ds \qquad (2.17)$$

$$\forall v \in V_\Omega$$

As shown above, the homogenized elastic constants can be computed within the basic

cell by solving the problem 2.14, and do not depend on the macroscopic deformation u^0.

If a composite material has a uniform cell structure in the whole domain Ω, the

microscopic problem 2.14 needs to be solved only once.

Following Sigmund (1994), equation (2.16) can be rewritten as

$$E_{ijkl}^H = \frac{1}{Y} \int_Y \left[E_{ijpq} - E_{ijpq} \varepsilon_{pq}^{*(kl)} \right] dY \qquad (2.18)$$

where $\varepsilon_{pq}^{*(kl)} = \partial \chi_p^{kl} / \partial y_q$ is still the solution to (2.14). Let now $\varepsilon_{pq}^{0(kl)}$ represent one of

three homogeneous tests strain-fields applied on the base cell, namely, two tensile strains

and one shear strain (Figure 2.3), i.e.,

$$\{\varepsilon^{01}\} = \begin{Bmatrix} 1 \\ 0 \\ 0 \end{Bmatrix} \quad \{\varepsilon^{02}\} = \begin{Bmatrix} 0 \\ 1 \\ 0 \end{Bmatrix} \quad \{\varepsilon^{03}\} = \begin{Bmatrix} 0 \\ 1 \\ 0 \end{Bmatrix} \qquad (2.19)$$
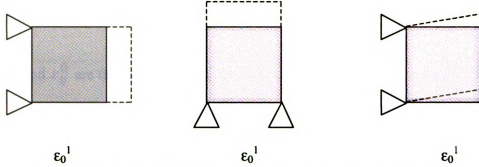
15

Figure 2.3. Model of the three-test strain used in homogenization

The solutions to problem (2.14) correspond to the deformation of the base cell, when subjected to the three independent cases of pre-strain $\{\varepsilon_0\}$ and periodic boundary conditions, and can be obtained numerically using a finite-element method. Homogenized elastic constants can be obtained by substituting the result of the finite-element analysis $\varepsilon_{pq}^{*(kl)}$ into (2.18).

In order to use a topology optimization method to find micro-geometries with prescribed effective constants, it is important to express the elastic constants E_{ijkl}^{H} in (2.18) in terms of element strain energies. This will make it possible to use the existing algorithms for the topology optimization. A homogenization method expressed in terms of element strain energies is described in the following.

Rewriting equation (2.18) we obtain

$$\varepsilon_{ij}^0 E_{ijkl}^H \varepsilon_{kl}^0 = \frac{1}{Y} \int_Y \left[(\varepsilon_{ij}^0 - \varepsilon_{ij}^*)^T E_{ijkl} (\varepsilon_{kl}^0 - \varepsilon_{kl}^*) \right] dY \qquad (2.20)$$

where ε_{kl}^0 and ε_{ij}^0 are the test strains field and ε_{ij}^* and ε_{kl}^* are the induced strains field

coming from the in-homogeneities of the microstructure . If the base cell is discretized by

N finite elements, the element mutual energy $Q_r{}^e$ in each element e, associated with test

strain field $\{\varepsilon_0\}$, can then be written as

$$Q_1{}^e = \frac{1}{Y^e} \int_{Y^e} \left[(\varepsilon_{e(1)}^0 - \varepsilon_{e(1)}^*)^T E_{ijkl} (\varepsilon_{e(1)}^0 - \varepsilon_{e(1)}^*) \right] dy^e \quad e=1,\ldots,N \qquad (2.21)$$

$$Q_2{}^e = \frac{1}{Y^e} \int_{Y^e} \left[(\varepsilon_{e(2)}^0 - \varepsilon_{e(2)}^*)^T E_{ijkl} (\varepsilon_{e(2)}^0 - \varepsilon_{e(2)}^*) \right] dy^e \quad e=1,\ldots,N \qquad (2.22)$$

$$Q_3{}^e = \frac{1}{Y^e} \int_{Y^e} \left[(\varepsilon_{e(3)}^0 - \varepsilon_{e(3)}^*)^T E_{ijkl} (\varepsilon_{e(3)}^0 - \varepsilon_{e(3)}^*) \right] dy^e \quad e=1,\ldots,N \qquad (2.23)$$

$$Q_4{}^e = \frac{1}{Y^e} \int_{Y^e} \left[(\varepsilon_{e(1)}^0 - \varepsilon_{e(1)}^*)^T E_{ijkl} (\varepsilon_{e(2)}^0 - \varepsilon_{e(2)}^*) \right] dy^e \quad e=1,\ldots,N \qquad (2.24)$$

$$Q_5{}^e = \frac{1}{Y^e} \int_{Y^e} \left[(\varepsilon_{e(2)}^0 - \varepsilon_{e(2)}^*)^T E_{ijkl} (\varepsilon_{e(3)}^0 - \varepsilon_{e(3)}^*) \right] dy^e \quad e=1,\ldots,N \qquad (2.25)$$

$$Q_6{}^e = \frac{1}{Y^e} \int_{Y^e} \left[(\varepsilon_{e(1)}^0 - \varepsilon_{e(1)}^*)^T E_{ijkl} (\varepsilon_{e(3)}^0 - \varepsilon_{e(3)}^*) \right] dy^e \quad e=1,\ldots,N \qquad (2.26)$$

where test strain field $\{\varepsilon_e^0\} = \{\varepsilon^0\}$; $\{\varepsilon_e^*\}$ is the induced train field in element e .

Since we assume that the base cell is discretized by N finite elements, we can sum the element strain energies to obtain the expression of each entry in the homogenized elastic tensor E^H.

$$E_r{}^H = \sum_{e=1}^{N} Q_r{}^e \qquad e=1,...,N \quad r=1,2,3,4,5,6 \qquad (2.27)$$

where we have used the following abbreviation

$$1111 \rightarrow 1 \quad 2222 \rightarrow 2 \quad 1212 \rightarrow 3$$
$$1122 \rightarrow 4 \quad 1112 \rightarrow 5 \quad 2212 \rightarrow 6$$

Now we only need to calculate each element strain energy Q_r^e from (2.21) to get the homogenized elastic constants of the composite material.

Chapter3

TILING OF 2-DIMENSIONAL DOMAINS USING POLYGON

In the previous derivation (Chapter 2), it is usually enough to use square cells only (i.e., Y is a square or a rectangle). However, base cells with more general shapes could lead to other interesting results. In this thesis, we use the topology optimization method to solve an inverse, homogenization problem with polygonal cells. For this purpose, Y needs to be defined so that it can tile the plane periodically. If Y is defined as a simple square or rectangle, this requirement can be easily met. When we allow the base cell to take a polygonal shape, this restriction is more difficult to impose.

We should review basic tiling concepts and introduce some basic results from Benard and Diaz (2001). We consider various shapes of cells capable of tiling the plane. Let T be a set of tiles in plane, which cover the plane without gaps or overlaps. T is a collection of tiles T_i. Here we only discuss periodic monohedral tilings which involve translations of a single polygonal proto-tile. All tiles have the same shape and size in monoheral tilings. In a periodic tiling, each set T_i is a tile. Every tile T_i in T has the form

$$T_i = P + md_1 + md_2$$

where P is the proto-tile, representative tile in monohedral tiling, m and n are integers and d_1 and d_2 are two non-parallel vectors called the tiling vector. The dependency of T on P, d_1 and d_2 will be expressed as $T(P, d_1, d_2)$.
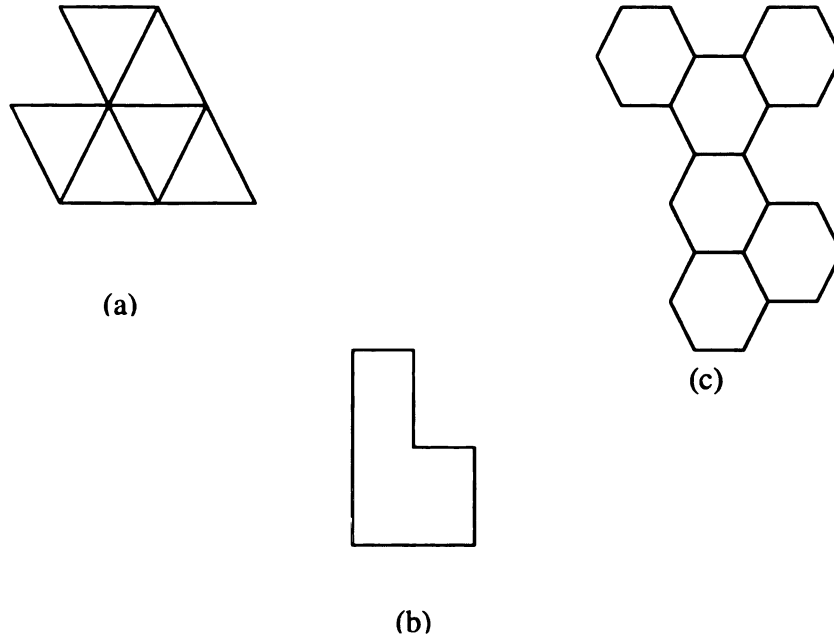
(a)

(b)

(c)

Figure 3.1. Examples of various prototiles:
(a) polyiamond (b)polyomino (c) polyhexe (Benard and Diaz
(2001))

Figure 3.1 shows several interesting examples of different proto-tile. The proto-tiles used

to tile the plane are polyiamond, L-shape, and polyhexe. These proto-tiles are made by

simply connecting the triangles, squares, and hexagons respectively.

We now introduce three important definitions leading to the concept of Y-periodicity

when Y is a polygon.

Definition: Lattice.

A lattice is a collection of translates of a single point $p \in P$ associated with a periodic tiling T along the tiling directions, i.e., the set of points

$$L(d_1, d_2) = \{q : q = p + md_1 + nd_2, m \quad and \quad n \quad are \quad Integers\}$$

Such lattice forms periodic parallelograms called fundamental domains, or fundamental parallelograms.
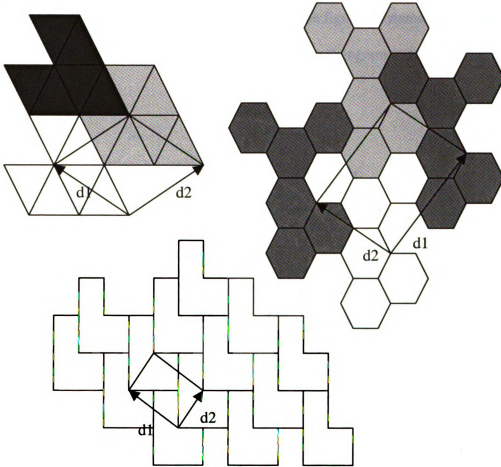
Figure 3.2. Fundamental domains associates with the tiling with polyiamond, polyhexe, and L-shape prototile (Benard and Diaz (2001))

Definition: Fundamental Domain.

A fundamental domain is any parallelogram F with its corners on the lattice $L(d_1,d_2)$, which tiles the plane with tiling vectors v_1 and v_2 and generate a lattice $L(v_1,v_2)$ equal to L.

There can be several fundamental domains associated with the same lattice. Figure 3.2 shows several examples of fundamental domain. In the figure polyiamond, polyhexe, and L-shape proto-tiles can be associated with different parallelogram individually.
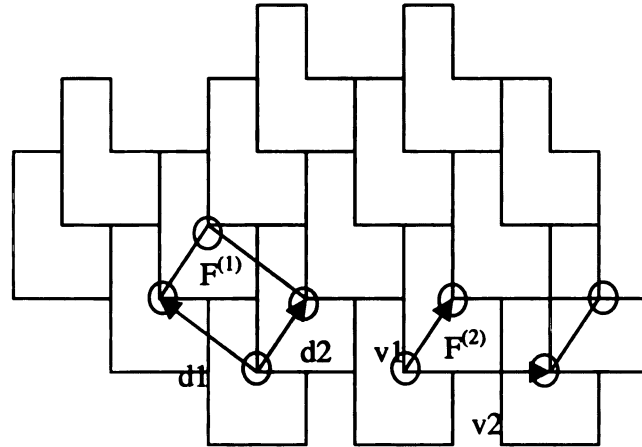
Figure 3.3. Fundamental domains associated with tiling of L-shape proto-tiles

Figure 3.3 shows a periodic tiling of L-shape proto-tiles. In the figure, two fundamental domains $F^{(1)}$ and $F^{(2)}$ associated with the same tiling, in which $L(p,d_1,d_2)$ and $L(p,v_1,v_2)$ are identical(the four points of the parallelograms $F^{(1)}$ and $F^{(2)}$ are the same points of the L-shape proto-tile).

Definition: T-periodic function.

A function $\Phi : R^2 \to R$ is $T(P)$-periodic, if $\Phi(p) = \Phi(p + md_1 + md_2)$ for all $p \in P$ and integers m and n.

A function Φ that is $T(P)$-periodic uses the base cell P in its definition. It can be very complicated to implement the numeric associated with the homogenization problem on such a base cell P. Figure 3.4 shows an example of a node numbering of a polyhexe base cell. In order to meet the periodic boundary conditions, the node numbers have to be
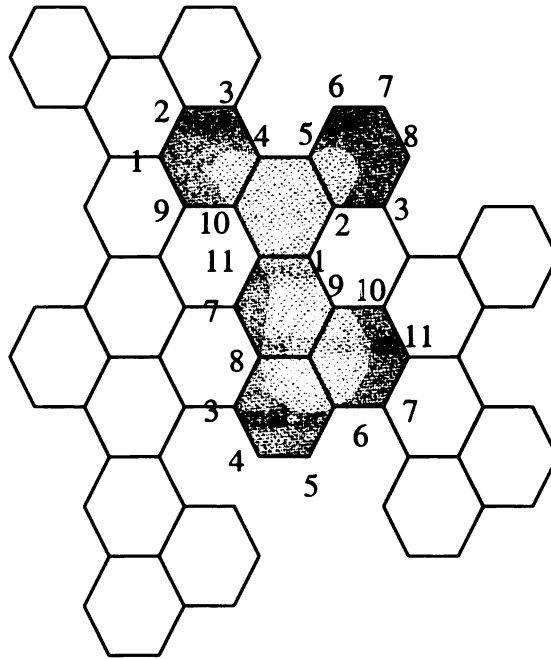

Figure 3.4. Periodic node numbering pattern of polyhexe proto-tile

assigned in the pattern shown in figure 3.4. If the shape of the base cell changes, the numbering of nodes will also need to be changed. This would be a very cumbersome procedure.

23

We can use a parallelogram as fundamental domain to avoid these difficulties. From the examples shown in Figure 3.2 and Figure 3.3, we can see that fundamental domains preserve the periodicity of $T(P)$-periodic function. Because proto-tile P and fundamental domain F are associated with the same lattice, a function that is $T(P)$-periodic is also $T(F)$-periodic. The material design problem then can use F instead of P as its base cell to solve the homogenization problem. So no mater how complex the polygonal base cell is, we can always find a fundamental domain to describe the periodicity of the problem. In others words, we can always use a parallelogram cell to solve the $T(P)$-periodic function in which P is a polygonal cell. This result will expand the design space of material design problems.

Figure 3.5 shows the geometry of a fundamental domain. A more complete parameterization of design space of material tensors can be achieved by including in the analysis the sides L_x/L_y and the internal angle α. One may also find interesting solutions that cannot be reached when the base cell is restricted to be rectangular.
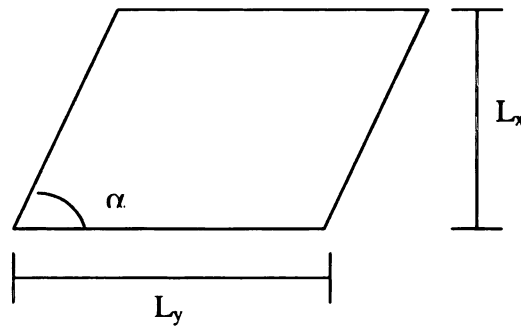
Figure 3.5. Definition of the parallelogram cell

As in Figure 3.2, no mater which kind of polygonal proto-tile is used to tile the plane, we

can always find a fundamental domain associated with it. After we transfer all these tiling

problems into a basic parallelogram problem, solving the parallelogram cell-tiling

problem can use a general routine.

Chapter 4

SOLVING THE INVERSE PROVLEM

In this chapter, the numerical approach for material design or inverse homogenization method is briefly reviewed. The method is then applied to the design of two-phase composites with mixtures characterized by a polygonal cell.

As stated in Chapter 3, the material microstructure is assumed to be periodic and fully described by its smallest repetitive base cell. In order to use the finite element method, the base cell is discretized by N finite elements. The effective properties are found by using the numerical homogenization method, which is stated in Chapter 2, using the finite element analysis to find the local fields and applying periodic boundary conditions.

In approaching the problem of getting the effective average elastic properties E^H of the base cell, the popular SIMP method, which is also used by Sigmund (1995), is used here. This method uses a variable thickness sheet formulation and penalized intermediate design values. The method assumes that the element elastic tensor E^e is isotropic and expressed as

$$E^e = \rho_e^p E^0 \qquad\qquad \rho_e \in (0,1] \qquad\qquad (4.1)$$

Here $\rho = \{\rho_1, ..., \rho_N\}$ are the design variables, and p is a real number, $p > 1$, used to

penalize the intermediate design values (i.e., values of ρ between 0 and 1). E^0 is an

isotropic reference tensor, which is expressed in the standard (matrix) engineering form,

$$\left[E^0\right] = \frac{E}{1-v^2} \begin{bmatrix} 1 & v & 0 \\ v & 1 & 0 \\ 0 & 0 & \frac{(1-v)}{2} \end{bmatrix} \tag{4.2}$$

where E is the modulus of elasticity and v is Poison's ratio. In terms of shear modulus

μ and bulk modulus k, the Young's modulus can be defined as

$$E = \frac{9k\mu}{3k + \mu} \tag{4.3}$$

and Poison's ratio can be defined as

$$v = \frac{1}{2}(\frac{3k - 2\mu}{3k + \mu}) \tag{4.4}$$

The isotropic reference tensor E^0 can also be expressed in terms of shear modulus μ

and bulk modulus k

$$\left[E^0\right] = \frac{\frac{9k\mu}{3k + \mu}}{1 - (\frac{3k - 2\mu}{6k + 2\mu})^2} \begin{bmatrix} 1 & \frac{3k - 2\mu}{6k + 2\mu} & 0 \\ \frac{3k - 2\mu}{6k + 2\mu} & 1 & 0 \\ 0 & 0 & \frac{(3k + 4\mu)}{12k + 4\mu} \end{bmatrix} \tag{4.5}$$

The inverse homogenization method is applied here to solve the following problem:

For a given amount of material, find the microstructure arrangement, which minimizes

the deviation from a target tensor E^*. In other words, in this material design problem, the

goal is to find a set of design variables $\rho = \{\rho_1,...,\rho_N\}$ that make the material effective

tensor match the target tensor as close as possible. In addition to ρ, we also introduce an

additional design variable, t, to scale the material effective tensor as a scaling parameter.

The optimization problem is written as

$$Find \quad \{\rho_1, \rho_2 ..., \rho_N\} \quad and \quad t \quad that \quad will: \quad (4.6a)$$

$$Min: \quad ER \quad\quad\quad (4.6b)$$

$$Subject \quad to \quad \sum_{e=1}^{N} A_e \rho_e = v_0 A$$
$$0 < \rho_{\min} \leq \rho_e \leq 1 \quad\quad (4.6c)$$

where ρ_e represents the design variables, in this case, the proportion of strong

constituent in each element; N is the total number of elements that are used to discretize

the base cell; ER is the deviation from the target tensor, which will be defined below;

A_e is the area of each element; v_0 is a prescribed volume fraction, a number between 0

and 1; A is the area of base cell; and $\rho_{\min}$ is a prescribed lower bound for ρ_e, a small

number (e.g., $\rho_{\min} = 0.001$).

The objective function used in (4.6) is the weighted mean square deviation between E^H,

the homogenized elastic tensor, and the target tensor E^*. It is expressed as

w

te

an

As

opt

the

whe

Usin

$$ER = \frac{1}{2} \sum_{I=1}^{6} w_I (tE_I^H - E_I^*)^2 \tag{4.7}$$

where compact notation E_I^H is used to denoted the six independent entries of the elastic

tensor using abbreviations

$$1111 \longrightarrow 11 \longrightarrow 1 \quad 2222 \longrightarrow 22 \longrightarrow 2 \quad 1212 \longrightarrow 33 \longrightarrow 3$$
$$1122 \longrightarrow 12 \longrightarrow 4 \quad 1112 \longrightarrow 13 \longrightarrow 5 \quad 2212 \longrightarrow 23 \longrightarrow 6$$

and w_I is a prescribed, non-negative weight factor (I=1,...,6); E^* is the target tensor.

As the function ER is an unconstrained, convex function of t for fixed ρ, we can get the

optimal value of t, t^*, by solving the equation $\dfrac{\partial ER}{\partial t} = 0$ to minimize ER. Using

$$\frac{\partial ER}{\partial t} = \sum_{I=1}^{6} E_I^H w_I (tE_I^H - E_I^*) \tag{4.8}$$

the minimizer is

$$t^* = \frac{c_1}{c_2} \tag{4.9}$$

where

$$c_1 = \sum_{I=1}^{6} E_I^* w_I E_I^H \qquad and \qquad c_2 = \sum_{I=1}^{6} E_I^H w_I E_I^H \tag{4.10}$$

Using the t^* in (4.5) and (4.6), the optimization problem is reduced to:

$$Find \qquad \{\rho_1, \rho_2 ..., \rho_N\} \qquad that \qquad will: \tag{4.11a}$$

$$Min: \qquad ER = \frac{1}{2} \sum_{I=1}^{6} w_I (t^* E_I^H - E_I^*)^2 \tag{4.11b}$$

We

can

whe

Defi

and

$$Subject \quad to \quad \sum_{e=1}^{N} A_e \rho_e = v_0 A \tag{4.11c}$$

$$0 < \rho_{\min} \le \rho_e \le 1$$

We also need to provide the gradient of the objective function ER. The gradient $\nabla_\rho ER$

can be calculated from equation (4.11b)

$$\nabla_\rho ER = \sum_{I=1}^{6} (\frac{\partial ER}{\partial E_I^H} \frac{dE_I^H}{d\rho} + \frac{\partial ER}{\partial t^*} (\frac{\partial t^*}{\partial c_1} \frac{\partial c_1}{\partial E_I^H} \frac{dE_I^H}{d\rho} + \frac{\partial t^*}{\partial c_2} \frac{\partial c_2}{\partial E_I^H} \frac{dE_I^H}{d\rho})) \tag{4.12}$$

where

$$\sum_{I=1}^{6} (\frac{\partial ER}{\partial E_I^H} \frac{dE_I^H}{d\rho}) = \sum_{I=1}^{6} w_I (t^* E_I^H - E_I^*) t^* \frac{dE_I^H}{d\rho} \tag{4.13}$$

$$\frac{\partial ER}{\partial t^*} = \sum_{I=1}^{6} w_I (t^* E_I^H - E_I^*) E_I^H \tag{4.14}$$

$$\sum_{I=1}^{6} (\frac{\partial t^*}{\partial c_1} \frac{\partial c_1}{\partial E_I^H} \frac{dE_I^H}{d\rho}) = \frac{1}{c_2} \sum_{I=1}^{6} w_I E_I^* \frac{dE_I^H}{d\rho} \tag{4.15}$$

$$\sum_{I=1}^{6} (\frac{\partial t^*}{\partial c_2} \frac{\partial c_2}{\partial E_I^H} \frac{dE_I^H}{d\rho}) = -\frac{2c_1}{c_2^2} \sum_{I=1}^{6} w_I E_I^H \frac{dE_I^H}{d\rho} \tag{4.16}$$

Define now W as a 6x6 diagonal matrix with weights w_I in the diagonal entries. If E^H

and E^* are written in column vector form equation (4.10) can be rewritten as

$$c_1 = E^{*^T} W E^H \quad and \quad c_2 = E^{H^T} W E^H \tag{4.17}$$

30

ar

v

Th

fro

Figu

prob

and (4.12) can be expressed as

$$\nabla_\rho ER = (t^* E^H - E^*)^T W (t^* I_{6\times 6} + E^H E_t^T W)\frac{dE^H}{d\rho} \qquad (4.18)$$

where

$$E_t = \frac{1}{c_2}(E^* - \frac{2c_1}{c_2}E^H) \qquad (4.19)$$

The vector of the differential $\dfrac{dE^H}{d\rho}$ can be easily computed as $\dfrac{\partial E^H}{\partial \rho_e}$ (for fixed strains)

from (2.20) and (2.21),

$$\frac{\partial E_{ij}^H}{\partial \rho_e} = \sum_{e=1}^{N} \frac{p\rho_e^{P-1}}{A_e} \int_{Y^e} (\varepsilon^i{}_{0e} - \varepsilon^i{}_e)^T E^0 (\varepsilon^j{}_{0e} - \varepsilon^j{}_e) dA^e \qquad i, j = 1,2,3 \, (4.20)$$

Figure 4.1 shows the flowchart of the procedure to solve the inverse homogenization

problem.

```
                    ┌──────────┐
                    │  Start   │
                    └──────────┘
                    ┌──────────┐
                    │ Initialize │
                    └──────────┘
```

Discretize the domain. Assign degrees of freedom consistent with periodicity.

Finite element analysis for calculating the (3) induced strain field associated with the (3) test train ε^0

Calculate the element strain energy and the constitutive parameters, using equations (2.21) and (2.22)

Solving the homogenization problem

Update the design variables ρ_e s using the method of moving asymptotes (Svanverg (1987))

No — Is the objective function ER not changing?

Yes

Plot out the figure for the result microstructure

Stop

Figure 4.1 Flowchart of the procedure to solve the inverse homogenization problem (Sigmund 1995)

Chapter 5

EXAMPLES

In this chapter, several examples are presented. The routine used to generate the result is developed on the base of last three chapters. Here we set the penalty parameter p in the SIMP model as 1. In all these examples, the reference material E^0 has the bulk modulus 1.333 and shear modulus 1. In example 1, 2 the volume v_0 is 0.45 and the lower limit of the strong material percentage of each element $\rho_{min} = 0.01$. Example 1 illustrates the existence of multiple solutions as the optimization starts from different starting point. Example 2 shows the effect of the shape of the fundamental domain on the solution. In Example 3, we study the effect of changing of the amounts of available material on the result obtained while keeping other parameters fixed. In Example 1, 2, and 3, the target tensor is defined as

$$\left[E^*\right] = \begin{bmatrix} 1 & 0.333 & 0 \\ 0.333 & 1 & 0 \\ 0 & 0 & 0.333 \end{bmatrix} \tag{5.1}$$

In Example 4, we will change the value of shear modulus μ and test the procedure to see whether we can approach the lower right corner of the Hashin-Shtrikman bounds (Figure 1.1) using a parallelogram base cell.

The inverse homogenization problem is solved by the method of moving asymptotes (Svanverg (1987)) and the filter is used as in Sigmund (1995). As discussed in Chapter 3, the homogenization problem in these examples is solved on the fundamental domain associated with the given proto-tile.

5.1 Example 1-effect of different starting point

In this example we will show that different starting points will lead to different answer with the same target tensor. The fundamental domain used here is a parallelogram with ratio $L_x / L_y = 1/3$ and the internal angle $\alpha = 45°$.

The result shows that the solution to the problem is not unique, and that convergence to a particular solution depends on the starting layout.

Figures 5.2, 5.4, and 5.6 show three solutions using the same target tensor (5.1). Figure 5.2 and 5.4 were obtained from a randomly chosen starting point (material distribution matrix). Figure 5.6 was obtained by setting the upper one fifth of material distribution matrix as $\rho = \rho_0$ and setting $\rho = 2\rho_0$ for the rest of the domain. As the figures show, the different starting points result in qualitatively different layouts, all of which produce the same effective tensor E^*.

Figure 5.1. Example1a base cell
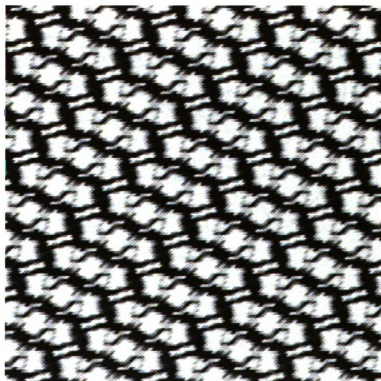
Figure 5.2. Example 1a solution

Figure 5.3. Example 1b base cell
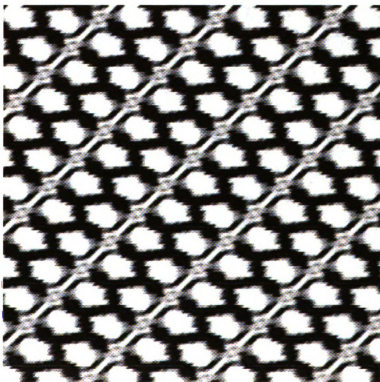
Figure 5.4. Example 1b solution

Figure 5.5. Example 1c base cell
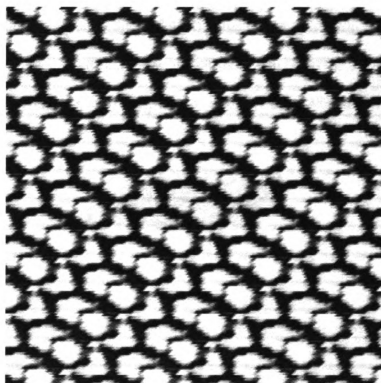
Figure 5.6. Example 1c solution

5.2 Example2-effect of different base cell geometry

In this example we will investigate whether different shape parallelograms can lead to different answers matching the same target tensor. So the shape of the fundamental domain will be changed in this example.

The results will be shown in two series. The first series will change the length ratio L_x/L_y, when the internal angle α remaining constant at $45°$. The second series will keep a constant length ratio $L_x/L_y=1$ and change internal angle α. As the results shown in Example 1, the starting guess has effect on the result. So we keep the starting guess same by setting the upper one fifth of material distribution matrix as $\rho = \rho_0$ and $\rho = 2\rho_0$ for other part in first series. In second series, we set starting guess as the upper one eighth of material distribution matrix as $\rho = \rho_0$ and $\rho = 2\rho_0$ for other part (shown in

Figure 5.7. Initial design of the parallelogram cell

Figure5.7). The results for fundamental domain with different length ratios and different internal angles are shown in Figure 5.8 to Figure 5.15. First four figures show the results of different length ratio, the length ratios are L_x/L_y =1, 1/2, 2/3, 2/5 respectively. The second four figure show the results of different angles, $45°, 60°, 75°$ and $90°$

38

individually. The results show that one can achieve different microstructures that match the desired target tensor by change the geometry of the base cell.
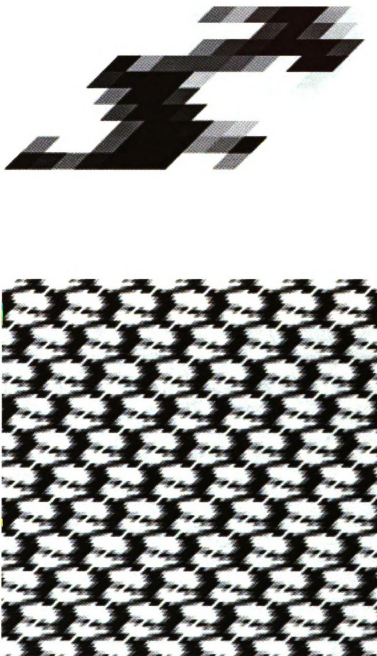
Figure 5.8. Example 2a L_x/L_y=1 cell and solution
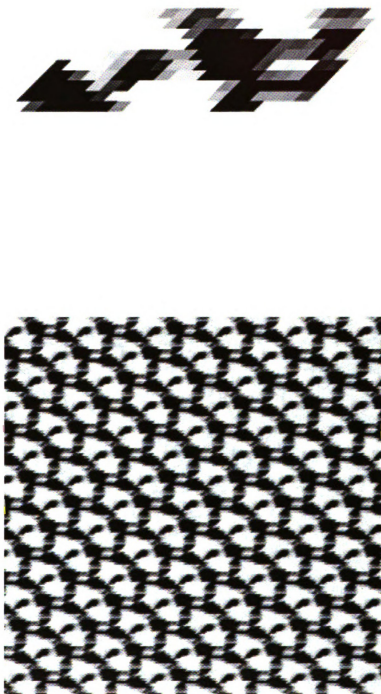
Figure 5.9. Example 2b L_x/L_y=1/2 cell and solution
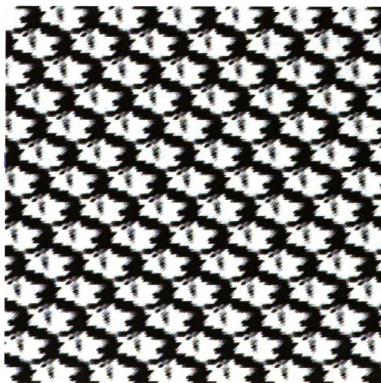
Figure 5.10. Example 2c L_x/L_y=2/3 cell and solution
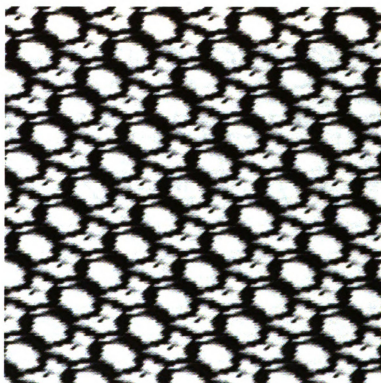
Figure 5.11. Example 2d $L_x/L_y=2/5$ cell and solution
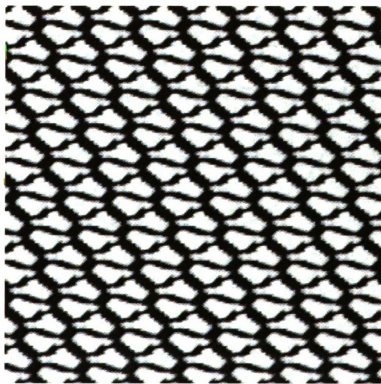
Figure 5.12. Example 2e α=45 cell and solution
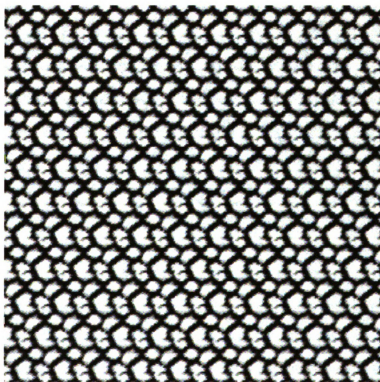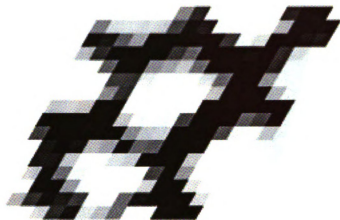
Figure 5.13. Example 2f α=60 cell and solution
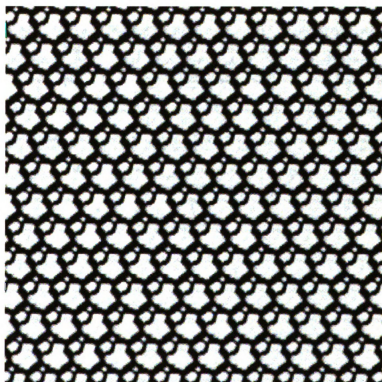
Figure 5.14. Example 2g α=75 cell and solution
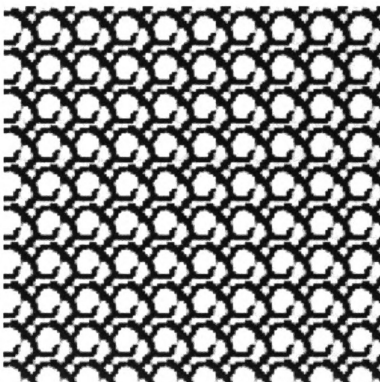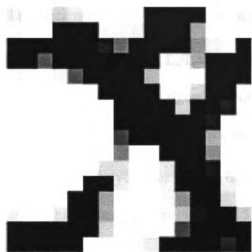
Figure 5.15. Example 2h α=90 cell and solution

5.3 Example3- effect of different strong material volume

In this example we will investigate that different volume v_0 can lead to different answer with same target tensor. All the parameters are fixed, except the percentage of strong material. First, we set the shape of parallelogram as $L_x/L_y=1$ and $\alpha = 75°$. The volumes are 0.2, 0.25, 0.3, 0.35, 0.4, 0.45, and 0.5. Since the figure for volume 0.45 has been shown in Figure 5.14, only the others will be shown here. Second, we set the shape of parallelogram as $L_x/L_y=1$ and $\alpha = 90°$. The volumes are 0.2, 0.3 and 0.45. For the same reason, the figure for volume 0.45 has been shown in Figure 5.15.

The results show it clearly that different volume of strong material can generate different answers that match the same prescribed elastic tensor. When comparing these results; we can observe that small changes in volume induce small changes in the solution.

Figure 5.24 shows the convergence curve of example 3a, 3c and 3e. From the figure we can see that the volume has no effect on the pattern of convergence. Also we can see that the objective function value converges rapidly after an initial "flat" period.

47
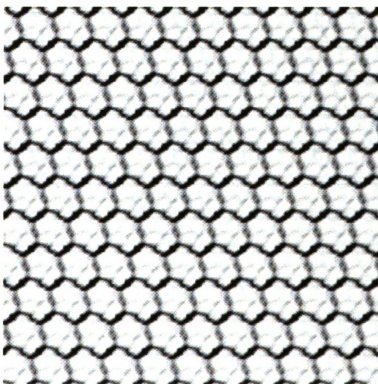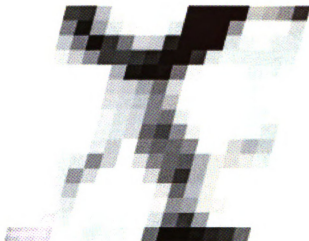
Figure 5.16. Example 3a L_x/L_y=1 $\alpha = 75°$ volume 0.2
cell and solution
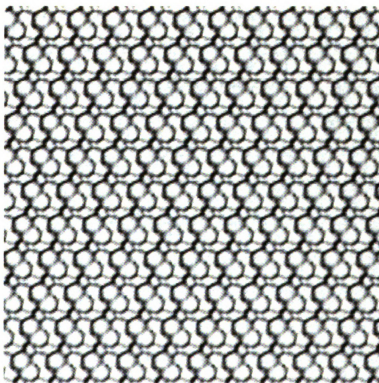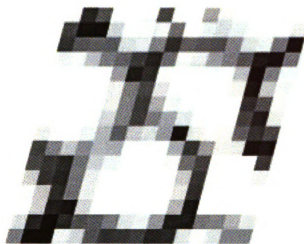
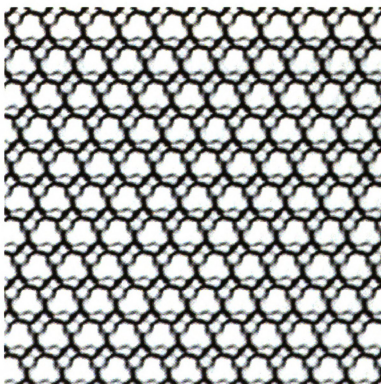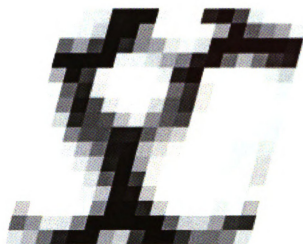Figure 5.17. Example 3b $L_x/L_y=1$ $\alpha = 75°$ volume 0.25
cell and solution

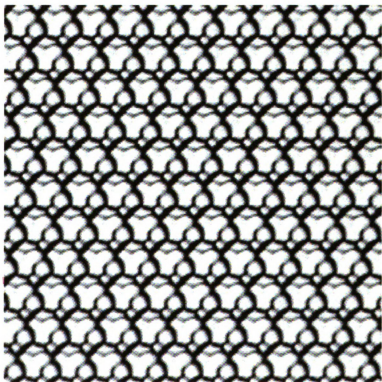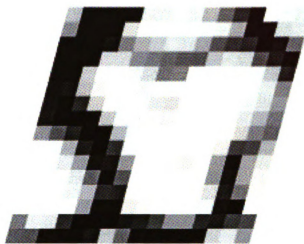Figure 5.18. Example 3c $L_x/L_y = 1$ $\alpha = 75°$ volume 0.3 cell and solution

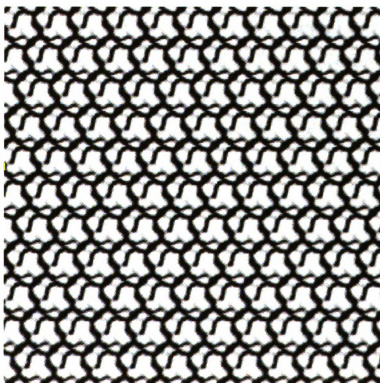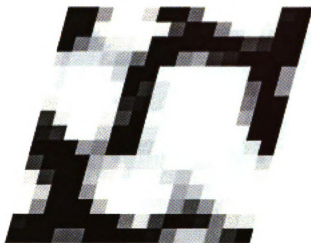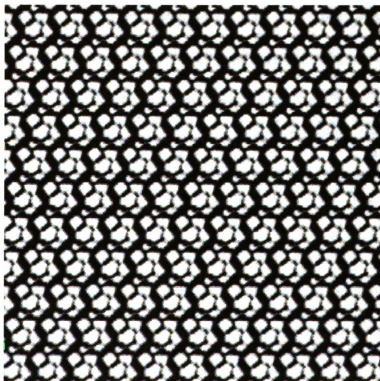Figure 5.19. Example 3d $L_x/L_y=1$ $\alpha = 75°$ volume 0.35
cell and solution

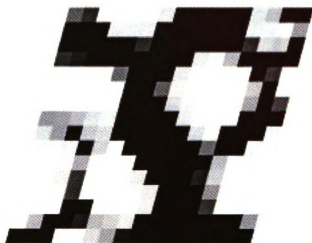Figure 5.20. Example 3e L_x/L_y=1 α = 75° volume 0.4 cell and solution

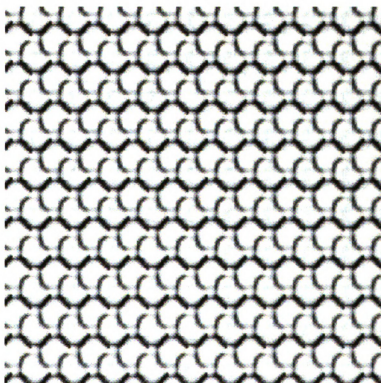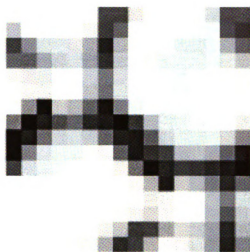Figure 5.21. Example 3f $L_x/L_y=1$ $\alpha = 75°$ volume 0.5 cell and solution

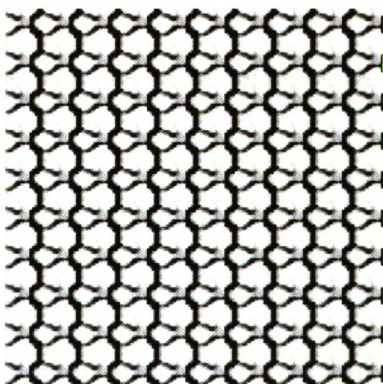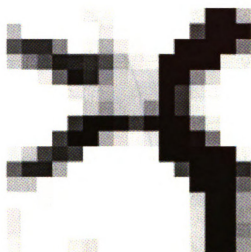Figure 5.22. Example 3g $L_x/L_y=1$ $\alpha = 90°$ volume 0.2 cell and solution

Figure 5.23. Example 3h $L_x/L_y=1$ $\alpha = 90°$ volume 0.3 cell and solution
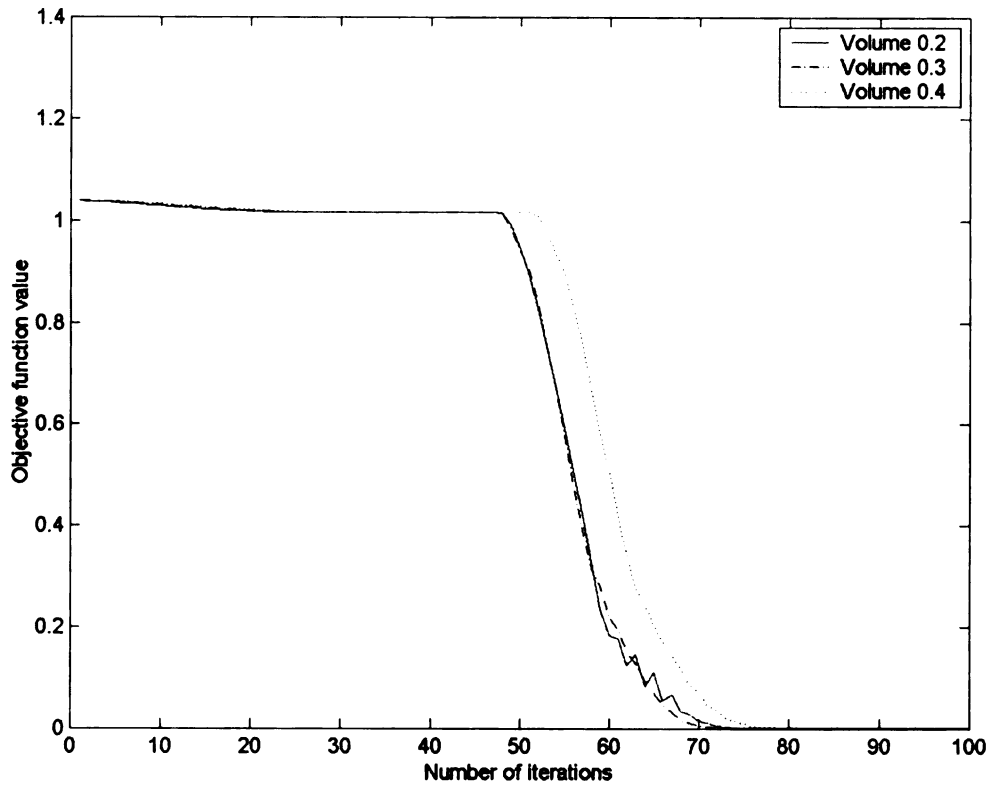
Figure 5.24. Convergence of the objective function with different strong material volume

5.4 Example 4- material with extreme property

In this example, we will present several solutions which approach the lower right corner

of Hashin-Shtrikman bounds for two-phase isotropic composites in well order case.

In well order case, the upper Hashin-Shtrikman bound of bulk modulus is defined as

$$k_u^{HS} = k^2 + \cfrac{1-\rho}{\cfrac{1}{k^1 - k^2} + \cfrac{\rho}{k^2 + \mu^2}} \tag{5.2}$$

and the lower Hashin-Shtrikman bound of shear modulus is defined as

$$\mu_l^{HS} = \mu^1 + \cfrac{\rho}{\cfrac{1}{\mu^2 - \mu^1} + \cfrac{(1-\rho)(k^1 + 2\mu^1)}{2\mu^1(k^1 + \mu^1)}} \tag{5.3}$$

where k^1, k^2, μ^1 and μ^2 denote the bulk moduli and shear moduli of two isotropic

constituents , ρ is the given volume fraction of strong material.

The improved lower Walpole bound of shear modulus is defined as

$$\mu_l^{WP} = \mu^1 + \cfrac{\rho}{\cfrac{1}{\mu^2 - \mu^1} + \cfrac{(1-\rho)(k^2 + 2\mu^1)}{2\mu^1(k^2 + \mu^1)}} \tag{5.4}$$

Here our goal is set as upper Hashin-Shtrikman bound of bulk modulus and lower

Walpole bound of shear modulus, which is the lower right corner of Figure 1.1. The

solutions here are generated by fixing the bulk modulus at the upper bound and

decreasing the shear modulus to approach the lower Walpole bound.

We set $\rho = 0.45$ and $k^2 = 1.333$, $k^1 = 0.01k^2$, $\mu^2 = 1$ and $\mu^1 = 0.01\mu^2$. From

equations (5.2) and (5.4), the values of the target bulk modulus and shear modulus are

$k^* = 0.3593$ and $\mu^* = 0.0257$.

We first start with $k^* = 0.3461$ and $\mu^* = 0.0516$. The geometry of the base cell is $L_x/L_y=1$ $\alpha = 90°$. The target tensor generated is

$$[E^*] = \begin{bmatrix} 0.1807 & 0.0775 & 0 \\ 0.0775 & 0.1807 & 0 \\ 0 & 0 & 0.0516 \end{bmatrix}$$ (5.5)

Figure 5.25 shows the result.

Figure 5.26 shows the result for $k^* = 0.3593$ and $\mu^* = 0.0357$. The geometry of the base cell also is $L_x/L_y=1$ $\alpha = 90°$. The target tensor generated is

$$[E^*] = \begin{bmatrix} 0.1303 & 0.0589 & 0 \\ 0.0589 & 0.1303 & 0 \\ 0 & 0 & 0.0357 \end{bmatrix}$$ (5.6)

Next step we set $k^* = 0.3593$ and $\mu^* = 0.0307$. This shear modulus is middle point

between $\mu^* = 0.0357$ and $\mu^* = 0.0257$ (the lower Walpole shear modulus). The target

tensor is

$$[E^*] = \begin{bmatrix} 0.1133 & 0.0519 & 0 \\ 0.0519 & 0.1133 & 0 \\ 0 & 0 & 0.0307 \end{bmatrix}$$ (5.7)

The geometry of the base cell also is $L_x/L_y=(3)^{(3/2)}/4$ and $\alpha = 79°$. The result is shown

in Figure 5.27.

Next step we set $k^* = 0.3593$ and $\mu^* = 0.0287$. The geometry of the base cell also is

$L_x/L_y=(3)^{(3/2)}/4$ and $\alpha = 79°$. The target tensor is

$$[E^*] = \begin{bmatrix} 0.1064 & 0.0491 & 0 \\ 0.0491 & 0.1064 & 0 \\ 0 & 0 & 0.0287 \end{bmatrix} \tag{5.8}$$

The result is shown in Figure 5.28.

We then have tried $k^* = 0.3593$ and $\mu^* = 0.0277$. But the result can not converge to the target tensor. So we set the $\mu^* = 0.0282$, which is the middle point between $\mu^* = 0.0287$ and $\mu^* = 0.0277$. The geometry of the base cell also is $L_x/L_y = (3)^{\wedge}(3/2)/4$ and $\alpha = 79°$.

The target tensor is

$$[E^*] = \begin{bmatrix} 0.1047 & 0.0483 & 0 \\ 0.0483 & 0.1047 & 0 \\ 0 & 0 & 0.0282 \end{bmatrix} \tag{5.9}$$

The result is shown in Figure 5.29.

Comparison of these figures indicates that when the material properties approach the goal, the structure of the material is much more close to a hexagon. In Sigmund (1999), he uses a hexagon shape for the cell as a starting point to get a new class of extremal composites.

Our routine generates the same trend in optimization. But still under the condition of the parameters we set, the optimization result cannot attain the theoretical value.

The crosses in Figure 5.30 denote the effective properties of the topology-optimized microstructure we get in this example.
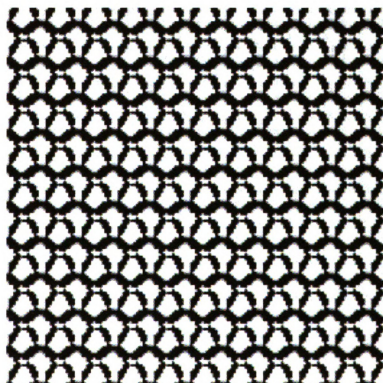
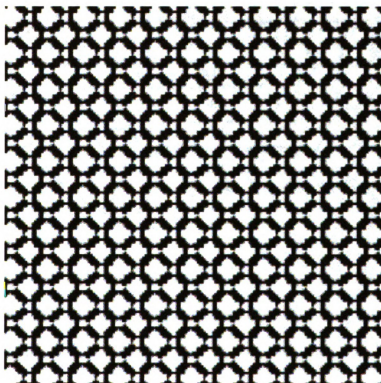Figure 5.25. Example 4a L_x/L_y=1 $\alpha = 90°$ cell and solution ($k^* = 0.3461$ and $\mu^* = 0.0516$.)

Figure 5.26. Example 4b L_x/L_y=1 $\alpha = 90°$ cell and solution ($k^* = 0.3593$ and $\mu^* = 0.0357$.)

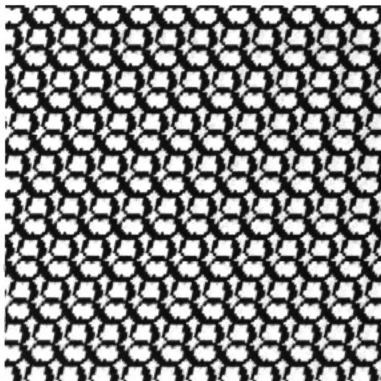Figure 5.27. Example 4c $L_x/L_y = (3)^{(3/2)}/4$ $\alpha = 79°$ cell and solution ($k^* = 0.3593$ and $\mu^* = 0.0307$)
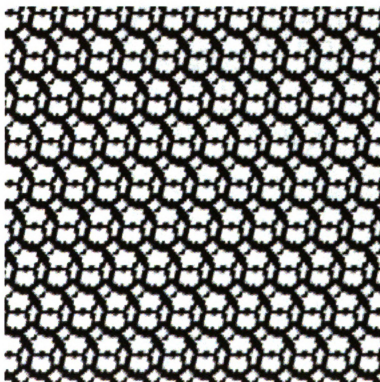
Figure 5.28. Example 4c $L_x/L_y=(3)^\wedge(3/2)/4$ $\alpha = 79°$ cell and solution ($k^* = 0.3593$ and $u^* = 0.0287$)
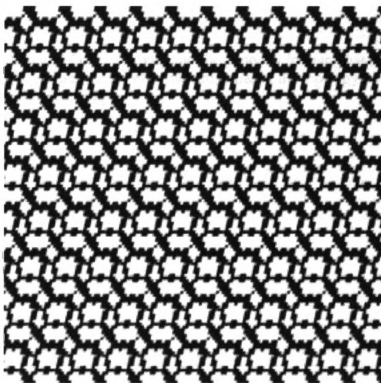
Figure 5.29. Example 4d $L_x/L_y=(3)^{(3/2)}/4$ $\alpha = 79°$ cell and solution ($k^* = 0.3593$ and $\mu^* = 0.0282$)
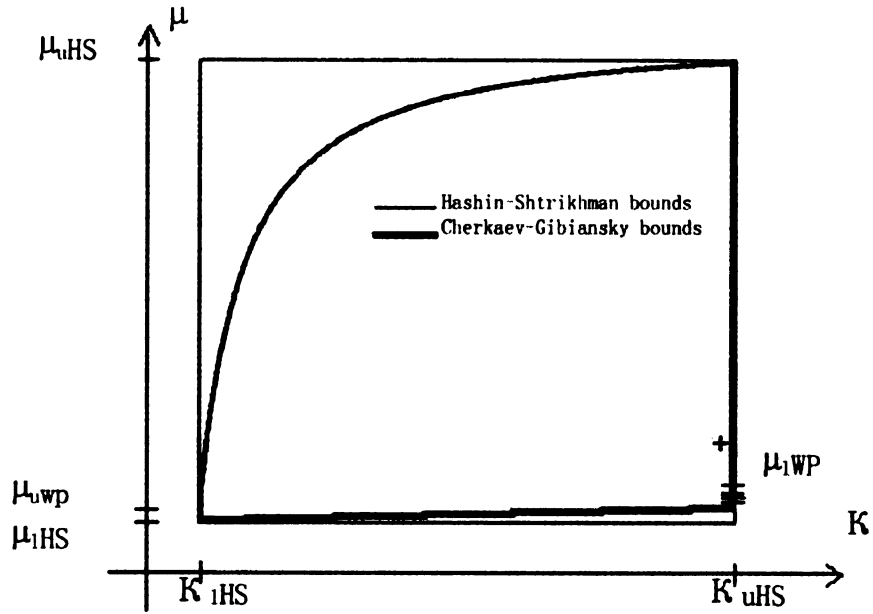
Figure 5.30. Bounds of effective bulk and shear moduli for two-phase isotropic composites. The crosses denote effective properties of the topology-optimized microstructures in Example 4.

Chapter 6

SUMMARY AND CONCLUSIONS

The inverse homogenization problem with polygonal cells has been successfully solved by topology optimization method by matching a target tensor. The effects of the initial material distribution, the shape of polygon cell and percentage of strong material on the solutions that match the same target tensor are studied. Besides these, material distributions approaching the lower right corner of Hashin-Shtrikman bound for well-order case have been found.

A summary of the results is presented below:

- Different starting points will lead to different answer with the same target tensor in the optimization procedure. Convergence to a particular solution depends on the initial material layout.

- One can achieve different microstructures that match the desired target tensor by changing the geometry of the base cell (parallelogram). This will expand the design space when compared to using only a rectangular cell.

- Different percentage of strong material can lead to different answer with same target tensor. Small changes in volume induce small changes in the solution. The volume has no effect on the pattern of convergence of the optimization problem.

- The results, which are generated for approaching the lower right corner of Hashin-Shtrikman bound for well-ordered case, show that more and more layers

in the bars of the hexagonal cell result in lower and lower shear modulus

(Sigmund 1999).

BIBLIOGRAPHY

Aboudi , J. "Mechanics of Composite Material". Amsterdam: Elsevier Science Publishers B.V 1991.

Benard, A., and A. R. Diaz. "On the discretization of problems involving periodic planar tilings". Commun.Numer.Meth.Engng (2001).

Ashby, M.F., and D.R.H. Jones, Engineering Materials 2, Oxford: Pergamon (1986).

Bendsoe, M.P., J.M. Guedes , R.B. Haber, P. Pedersen , and J.E. Taylor. "An Analytical Model to Predict Optimal Material Properties in the Contest of Optimal Structure Design". J.Appl.Mech. 61(3), (1994),930-937

Bendose, M.P., N. Kikuchi. "Generating optimal topologies in optimal design using a homogenization method". Computational Methods in Applied Mechanics and Engineering. 71 (1988), 197-224

Berryman, J.G., and G.W. Milton. "Microgeometry of random composites and porous media ". Journal of Physics D: Applied Physics. 21 (1988), 87-94.

Cherkaev, A.V., and L.V. Gibiansky. "Coupled estimates for the bulk and shear moduli of a two dimentional isotropic elastic composite". Journal of the Mechanics and Physics of Solid. 41(5), (1993), 937-980.

Crolet, J.M., B. Aoubiza, and A. Meunier. "Compact bone: Numerical simulation of mechanical characteristics". Journal of Biomechanics, v 26, n 6, Jun, 1993, p 677-687.

Francfort, G., and F. Murat. "Homogenization and optimal bounds in linear elasticity". Archives of Rational Mechanics Analysis 94 (1986),307-334.

Grabovsky, Y., and R.V. Kohn. "Microstructures minimizing the energy of a two phase elastic composite in two space dimensions. II: The Vigdergauz microstructure". Journal of the Mechanics and Physics of solids 43(6), (1995), 949-972.

Guedes, J.M., and N. Kikuchi. "Preprocessing and Postprocessing for Materials Based on the Homogenization Method with Adaptive Finite Element Method". Comp. Meth. Appl. Mech. Eng.Vol.83 (1990), 143-198.

Hashin, Z. "The elastic moduli of the heterogeneous materials". ASME Journal of Applied Mechanics 29 (1962), 143-150.

Hashin, Z. " Theory of composite materials". Mechanical of Composite Materials, F.W.Wend, H.Liebowitz and N.Perrone, eds. Oxford, Pergamon. (1970)

Hashin, Z., and S. Shtrikman. "A variational approach to the theory of the elastic behaviour of multiphase materials". Journal of the Mechanics and Physics of Solids (1963), 127-140

Hill, R. " The elastic behavior of the crystalline aggregate". Proceedings of the Royal Society of London A65 (1952), 349-354

Lions, J.L. "Some Methods in the Mathematical Analyses of System and their Control". New York: Gordon and Breach 1981

Lutie, K.A. , and A.V. Cherkaev . "The problem of formation of an optimal isotropic multi-component composite". Technical report 895.A.F.Ioffe Physical Technical Institute, Acad. Sci. of the USSR, Leningrad (1984). Shorter version in J.opt.Th. Appl 46 (1985), 571-589.

Milton, G.W. "Composite materials with Poisson's ratios close to -1". Journal of the Mechanics and Physics of Solids 40(5) (1992),1105-1137.

Milton, G.W., and A.V. Cherkaev. "Which elasticity tensors are realizable?". Journal of Engineering Materials and Technology, Transactions of theASME 117(4)(1995), 483-493.

Milton, G.W., and N. Phan-Thien. "New bounds on the effective elastic moduli of two-component materials ". Proceedings of the Royal Society of London A380 (1982), 305-331.

Oleinik, O.A. "On homogenization problems". Trends and Applications of Pure Mathematics to Mechanics, P.G. Ciarlet and M. Rouseau,eds., Berlin: Springer 1984.

Sigmund, O. "Materials with Prescribed Constitutive Parameters; An Inverse Homogenization Problem". DCAM Report 470, Technical University of Denmark 1993.

Sigmund, O. "Tailoring Materials with Prescribed elastic Properties". DCAM Report 480, Technical University of Denmark 1994.

Sigmund, O. " A new class of extremal composites". Journal of the Mechanics and Physics of Solids 48 (1999), 397-428.

Svanverg, K. "The method of moving asymptotes". Int. J. Num. Meth. Eng. 24 (1987), 359-373

Vigdergauz, S.B. "Energy-minimizing inclusions in a planar elastic structure with macro-isotropy". Structure Optimization 17(203), (1999), 104-112.

Walpole, L.J. "On bounds for the overall elastic moduli of inhomogeneous systems-I". J. Mech. Phys. Solids. Vol.14 (1966), 151-162.